Check for updates

A Journal of the Gesellschaft Deutscher Chemiker

Angewandte International Edition GDCh Chemie

www.angewandte.org

Accepted Article

Title: A Systematic Study of Methyl Carbodithioate Esters as Effective Gold Contact Groups for Single-Molecule Electronics

Authors: Jonathan Ward, Andrea Vezzoli, Charlie Wells, Steven Bailey, Samuel P Jarvis, Colin J Lambert, Craig Robertson, Richard Nichols, and Simon Higgins

This manuscript has been accepted after peer review and appears as an Accepted Article online prior to editing, proofing, and formal publication of the final Version of Record (VoR). The VoR will be published online in Early View as soon as possible and may be different to this Accepted Article as a result of editing. Readers should obtain the VoR from the journal website shown below when it is published to ensure accuracy of information. The authors are responsible for the content of this Accepted Article.

To be cited as: *Angew. Chem. Int. Ed.* **2024**, e202403577

Link to VoR: https://doi.org/10.1002/anie.202403577

WILEY VCH

10.1002/anie.202403577

15213773, ja, Downloaded from https://onlinelibrary.wiley.com/doi/10.1002/anie.202403577 by Lancaster University, Wiley Online Library on [31/05/2024]. See the Terms and Conditions (https://onlinelibrary.wiley.com/terms-and-conditions) on Wiley Online Library for rules of use; OA articles are governed by the applicable Creative Commons License

Accepted Manuscript

A Systematic Study of Methyl Carbodithioate Esters as Effective Gold Contact Groups for Single-Molecule Electronics

Jonathan S. Ward *[a,b], Andrea Vezzoli [a], Charlie Wells [c], Steven Bailey [c], Samuel P. Jarvis [c], Colin J. Lambert [c], Craig Robertson [a], Richard J. Nichols [a], and Simon J. Higgins[a]

[a] Department of Chemistry, University of Liverpool, Crown St., Liverpool, L69 7ZD, UK

[b] Chemistry Department, Lancaster University, Bailrigg, Lancaster, LA1 4YB, UK

[c] Physics Department, Lancaster University, Bailrigg, Lancaster, LA1 4YW, UK

E-Mail: j.ward10@lancaster.ac.uk

Keywords: Molecular electronics, Surface Chemistry, Material Science,

Abstract

There are several binding groups used within molecular electronics for anchoring molecules to metal electrodes (e.g., R–SMe, R–NH_2, R–CS_2^-, R–S^-). However, some anchoring groups that bind strongly to electrodes have poor/unknown stability, some have weak electrode coupling, while for some their binding motifs are not well defined. Further binding groups are required to aid molecular design and to achieve a suitable balance in performance across a range of properties. We present an in-depth investigation into the use of carbodithioate esters as contact groups for single-molecule conductance measurements, using scanning tunnelling microscopy break junction measurements (STM-BJ) and detailed surface spectroscopic analysis. We demonstrate that the methyl carbodithioate ester acts as an effective contact for gold electrodes in STM-BJ measurements. Surface enhanced Raman measurements demonstrate that the C=S functionality remains intact when adsorbed on to gold nanoparticles. A gold(I) complex was also synthesised showing a stable C=S→Au^I interaction from the ester. Comparison with a benzyl thiomethyl ether demonstrates that the C=S moiety significantly contributes to charge transport in single-molecule junctions. The overall performance of the CS_2Me group demonstrates it should be used more extensively and has strong potential for the fabrication of larger area devices with long-term stability.

Introduction

Our understanding of how to design molecules that efficiently conduct electricity across a nanogap in a molecular junction (metal-molecule-metal) configuration has increased dramatically in the past 15 years.[1-7] The contact groups are a fundamental part of the design of molecular wires, providing chemical, mechanical and electronic coupling of the molecular species to the electrodes. The same molecular backbone can show remarkably different

This article is protected by copyright. All rights reserved.

15213773, ja, Downloaded from https://onlinelibrary.wiley.com/doi/10.1002/anie.202403577 by Lancaster University, Wiley Online Library on [31/05/2024]. See the Terms and Conditions (https://onlinelibrary.wiley.com/terms-and-conditions) on Wiley Online Library for rules of use; OA articles are governed by the applicable Creative Commons License

Accepted Manuscript

conductance profiles with different electrode contact groups,[8] and a deeper understanding of this behaviour requires substantial further study, for instance through the characterisation of wider libraries of regularly used contact groups. Thiol contact groups have been used extensively in molecular electronics due to their high affinity for gold surfaces and the strong, covalent Au–S bond formed following surface interaction (of energy easily surpassing 1 eV).[9-12] Thiol-based molecules are particularly effective for monolayer fabrication, with the strong Au-S surface binding promoting the diffusion of gold atoms across the substrate surface.[13, 14] Thiol contact groups can however be problematic for scanning tunnelling microscopy break junction measurements, particularly under air, due to potential oxidation of the sulfur contact groups (among a number of other unwanted side reactions such as disulfide formation), and multiple anchoring configurations.[15-19] Thioether contact groups have been an excellent alternative contact group for gold substrates owing to their increased chemical stability, reasonable Au binding strength (0.5 – 0.8 eV) and preference for binding to undercoordinated Au atoms.[20] The main thioether contact groups that been used are methyl thioether[21-23] and benzodihydrothiophene.[23-26] While thioether contacts maintains good binding strength to gold, the coupling to the electrodes is not as efficient as with thiols due to the dative vs. covalent bond formed. Less efficient binding group–electrode coupling can also be observed with other dative-binding contact groups, such as pyridyl and amine.[24, 27] While amine contacts can be typically stable on alkyl functionality, stability issues have also been noted with aromatic amine functionality,[16] with oxidation products forming radicals.[28, 29] Therefore, to further advance molecular electronics it would be highly advantageous to have additional contact groups with clear supporting evidence of chemical stability, strong coupling to the electrodes and ease of synthesis, without the need for deprotection. We have been particularly interested in the use of carbodithioate esters as Au contact groups for single-molecule conductance measurements due to promising results with carbodithioate anions and dithiocarbamates.[30, 31] Carbodithioate anions were investigated previously by Bourget and co-workers where the 2-(trimethylsilyl)ethyl ester moiety was used as a protecting group for a carbodithioate ($R–CS_2^-$) contact group,[32] and interestingly, they demonstrate that the C=S functionality gives high conductance highlighting the utility of this group following the deliberate cleavage of the ester functionality. The single-molecule conductance of pristine carbodithioate esters (*i.e.* no conversion to the carbodithioic acid or anionic species) has not been investigated. Sodium dithiocarbamates have also been investigated as contact groups in larger area junctions and were shown to exhibit high conductance. [31]

Since initial investigations on $R–CS_2^-$,[30, 32] there has been a proliferation in the use of STM-BJ instrumentation, with an increasing focus on collecting large datasets and relying on good surface anchoring groups to achieve high quality electrical characterisation. With current

This article is protected by copyright. All rights reserved.

10.1002/anie.202403577

15213773, ja, Downloaded from https://onlinelibrary.wiley.com/doi/10.1002/anie.202403577 by Lancaster University, Wiley Online Library on [31/05/2024]. See the Terms and Conditions (https://onlinelibrary.wiley.com/terms-and-conditions) on Wiley Online Library for rules of use; OA articles are governed by the applicable Creative Commons License

Accepted Manuscript

equipment, typically, thousands of STM-BJ traces are collected to ensure robust statistical information on all possible binding modes are collected, which is typically significantly higher than what was typically collected >10 years ago due to advances in data collection and data handling. Taking inspiration from the prior work on other carbodithioate functionality, we postulated that carbodithioate esters themselves could act as effective gold contacts without the need for deprotection/chemical change or the presence of associated counterions/released protecting groups that could complicate the system. We postulated that a carbodithioate methyl ester might remain completely intact and retain the S–Me functionality that grants chemical stability to thioethers and that the C=S functionality could provide additional coupling strength making it appealing for detailed systematic investigation into carbodithioate esters as anchoring groups. As a result, we have synthesised a series of molecular wires with R–CS_2Me contact groups to verify their suitability for the fabrication of electrically transparent, strong, and stable molecular junctions.

The work presented in this manuscript demonstrates that carbodithioate esters are effective contact groups for molecular electronics with effectively 100% junction formation probability (JFP) even at very low (1 μM) solution concentrations (**Figure S24**). We demonstrate long-term stability of the R–CS_2Me functionality in the solution state under ambient conditions. Control experiments demonstrate that the presence of the C=S functionality compared to the benzyl methyl thioether equivalent boosts the conductance by approximately one order of magnitude, with a competitive conductance compared to other contacting groups which are used routinely in the field. Crucially, further investigations with Raman spectroscopy, X-ray photoelectron spectroscopy (XPS) and complexation with Au(I) salts show that carbodithioate esters remain intact when on the gold surface. We also show that terminating molecular wires with the carbodithioate methyl ester functionality is synthetically accessible through Pd-catalysed cross-coupling reactions. The strong binding of this functional group to the surface is supported by DFT calculations with binding energies to Au surfaces of (1–1.3 eV, which is comparable to that of a Au-S thiol interaction and stronger than other dative binding groups. This work clearly demonstrates that carbodithioate esters are a useful functionality, likely to become a commonly used motif as part of a molecular electronics toolbox, since they show a good balance of properties including defined and competitive conductance values, good stability including resistance to oxidation, good synthetic accessibility, known coordination to gold through spectroscopic characterisation and the absence of multiple conductance values.

This article is protected by copyright. All rights reserved.

10.1002/anie.202403577

15213773, ja, Downloaded from https://onlinelibrary.wiley.com/doi/10.1002/anie.202403577 by Lancaster University, Wiley Online Library on [31/05/2024]. See the Terms and Conditions (https://onlinelibrary.wiley.com/terms-and-conditions) on Wiley Online Library for rules of use; OA articles are governed by the applicable Creative Commons License

Accepted Manuscript

Results and discussion

Molecular design and synthesis

This work initially required the development of a series of molecular wires containing carbodithioate ester functionality that would enable detailed study of the contact group in STM-BJ experiments with the support of detailed surface characterisation (**Figure 1**). Aromatic and OPE functionality was selected for our molecular wires as these motifs are generally well studied and understood, placing the series in a molecular space where the carbodithioate ester can be appropriately compared to other functional groups used within molecular electronics.

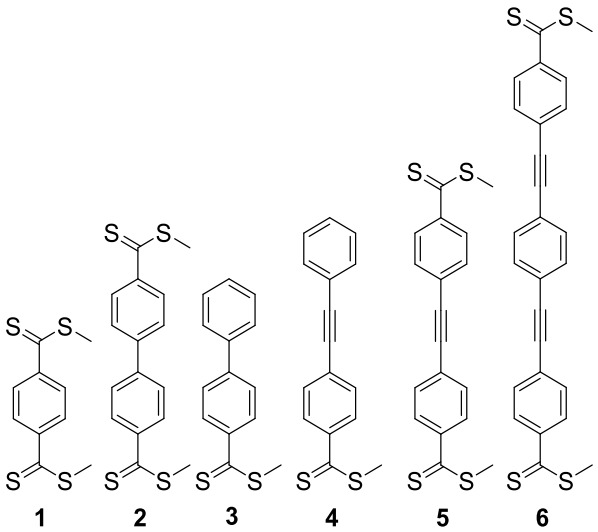

Figure 1. Carbodithioate ester containing molecular series prepared in this work.

The series in **Figure 1** contains molecular wires of varying molecular length with two carbodithioate ester groups for STM-BJ measurements (**1**, **2**, **5** and **6)**, and mono-carbodithioate ester functionality (**3** and **4**) specifically prepared for surface Raman measurements. **Scheme 1** shows an example synthetic strategy used to prepare alkyne-containing molecular wire **5**.

This article is protected by copyright. All rights reserved.

10.1002/anie.202403577

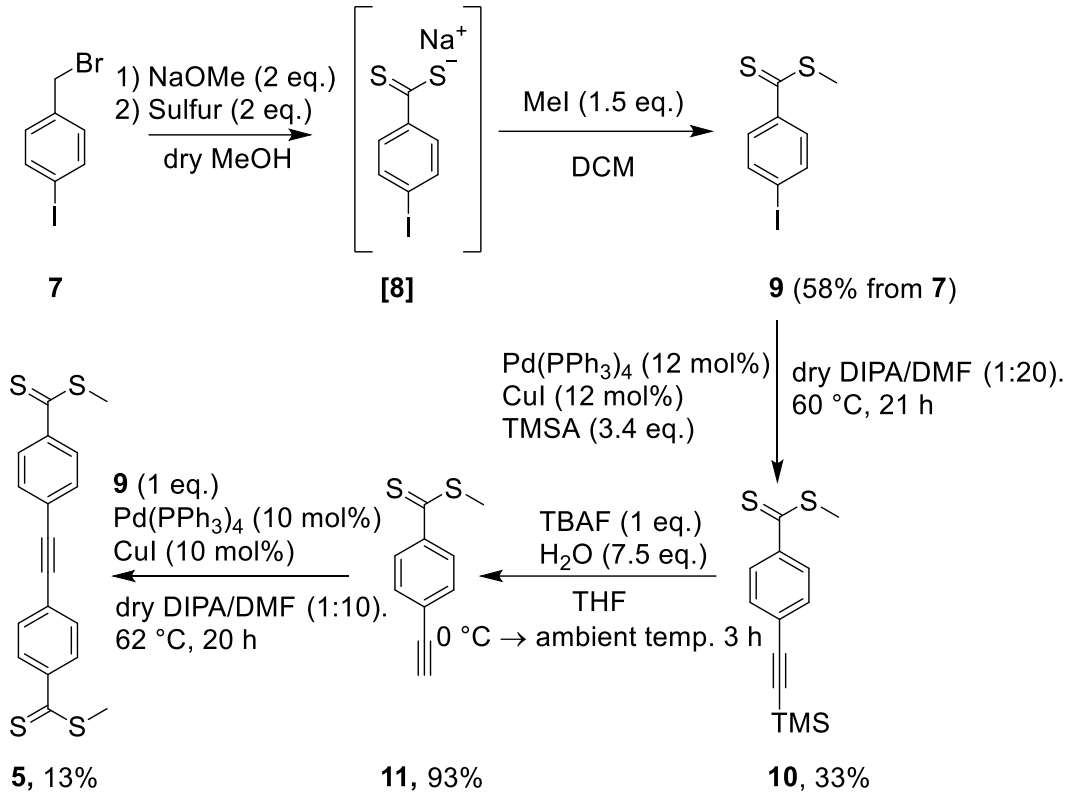

Scheme 1. Synthetic pathway to alkyne-containing molecular wire **5**.

Sodium carbodithioate functionality in this work was installed by treatment of benzyl halides with NaOMe (prepared *in-situ* by treating methanol with Na metal) and elemental sulfur.[33] Sodium intermediate **[8]** was treated with MeI in DCM to give the carbodithioate ester **9**. To make **5**, terminal alkyne-containing **11** was required for the appropriate Sonogashira cross-coupling with **9**. **11** was prepared by Sonogashira coupling of **9** with trimethylsilyl acetylene (TMSA) and subsequent deprotection with TBAF. The final Sonogashira coupling to yield **5** was performed using conditions reported by Therien and co-workers, which is one of the few reported cross-coupling transformations to tolerate the CS_2R functionality.[34] Similar conditions were used to prepare the other carbodithioate ester-containing compounds in the series as detailed in the supporting information section 1.

Scanning Tunnelling Microscopy-Break Junction Measurements.

The conductance of carbodithioate esters **1**–**2**, and **5**−**6** were measured using STM-BJ with an anisole solution of the target molecular wire (**Figure 2**).[35] In this technique, molecular junctions are fabricated between an Au tip and an Au substrate in a scanning tunnelling microscope. A 0.3 V bias is applied across the junction and the current is monitored as a function of the distance between the two electrodes. Details about the technique and the instrumentation used can be found in our previous publications on the subject.[36] For the measurement of the compounds presented in this study, relatively low concentrations (≤10 μM) were required to

This article is protected by copyright. All rights reserved.

15213773, ja, Downloaded from https://onlinelibrary.wiley.com/doi/10.1002/anie.202403577 by Lancaster University, Wiley Online Library on [31/05/2024]. See the Terms and Conditions (https://onlinelibrary.wiley.com/terms-and-conditions) on Wiley Online Library for rules of use; OA articles are governed by the applicable Creative Commons License

Accepted Manuscript

10.1002/anie.202403577

15213773, ja, Downloaded from https://onlinelibrary.wiley.com/doi/10.1002/anie.202403577 by Lancaster University, Wiley Online Library on [31/05/2024]. See the Terms and Conditions (https://onlinelibrary.wiley.com/terms-and-conditions) on Wiley Online Library for rules of use; OA articles are governed by the applicable Creative Commons License

Accepted Manuscript

consistently acquire high quality data. A piezo ramp of 20 nm was required to continuously refresh the tip during extension and retraction cycles of the STM-BJ measurement. >5000 traces were acquired for each target compound to obtain a statistically significant distribution of conductance data, analysed in the form of 1D histograms and 2D density maps. Occasional manual piezo control pushing the tip 50–100 nm in to the surface was required to clean the STM tip. It is possible that at concentrations ≥ 100 μM, high surface coverage with organic molecular wire occurs very rapidly, and this could explain why it is difficult to obtain single-molecule junctions at higher concentrations. Anisole was found to be an excellent solvent for measuring these molecules ensuring a consistent environment across the whole series and allowing us to overcome difficulties with mesitylene and mesitylene:tetrahydrofuran mixtures (large proportions of tetrahydrofuran can etch the Au substrate).[37] In mesitylene:tetrahydrofuran mixtures the repeatable formation of junctions to obtain enough reliable traces did not occur. The automated retraction and approach of the tip had to be repeatedly paused and moved to a new area on the surface making the measurement difficult. In anisole these difficulties were significantly suppressed and measuring 5000 traces was possible within a couple of hours.

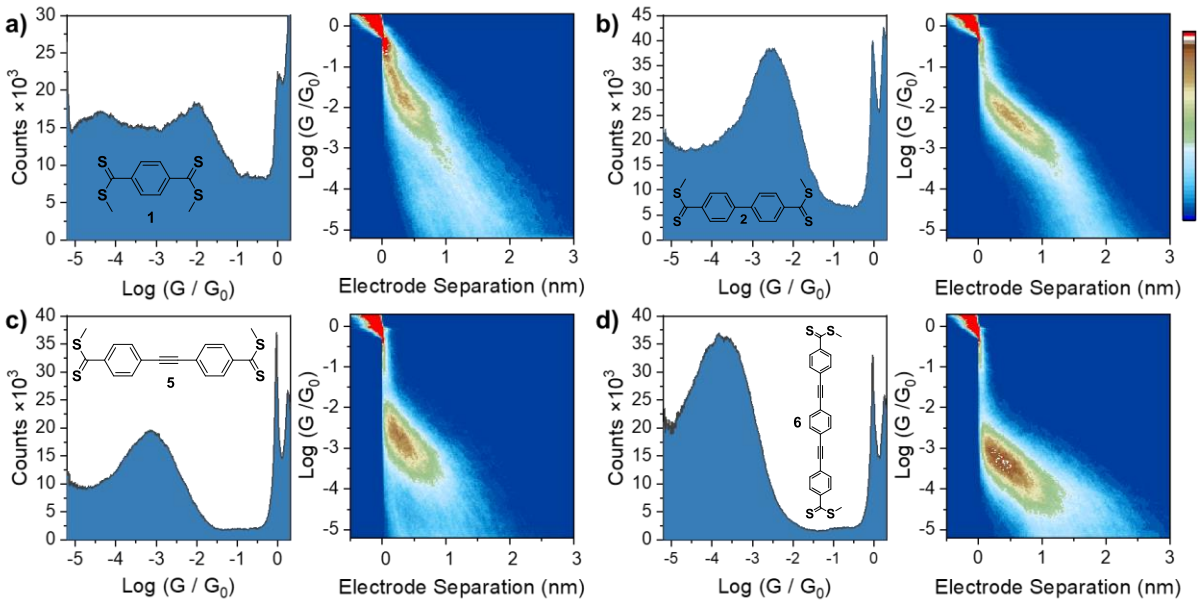

Figure 2. Scanning tunnelling microscopy break-junction measurements for a) **1,** b) **2**, c) **5** and d) **6** in anisole solvent at 10 μM for **1**−**2** and 1 μM for **5**–**6**. Further details: 300 mV bias, 20 nm piezo ramp.

STM-BJ results (**Figure 2**) show carbodithioate esters act as effective anchors to the gold electrodes. Clear conductance peaks are observed in the 1D histograms with high counts at the peak centre, and the 2D histograms demonstrate good general agreement of junction elongation with molecular length. Compound **2** shows low counts of junction elongation beyond the theoretical junction length at 10 μM. Measurement at 1 μM is in better agreement with the

This article is protected by copyright. All rights reserved.

10.1002/anie.202403577

15213773, ja, Downloaded from https://onlinelibrary.wiley.com/doi/10.1002/anie.202403577 by Lancaster University, Wiley Online Library on [31/05/2024]. See the Terms and Conditions (https://onlinelibrary.wiley.com/terms-and-conditions) on Wiley Online Library for rules of use; OA articles are governed by the applicable Creative Commons License

Accepted Manuscript

molecular length (**Figure S23** in SI). It is possible that with **2**, a small proportion of traces extend beyond the molecular length due to intermolecular stacking, thereby forming supramolecular 1:1 complexes of greater length. Compound **1** was also challenging to measure due to the short molecular length relative to the gold snapback distance and could only be measured at 10 μM. Higher and lower concentrations of **1** failed to yield sufficiently high-quality traces. Compounds **5**–**6** had to be measured at 1 μM to collect the 5000 traces required. Unsupervised data clustering on the STM-BJ data of compound **6** (**Figure S24**) reveals with a high degree of confidence that the JFP is effectively 100%, highlighting the ability of the carbodithioate ester functionality to bind to and form junctions efficiently at gold interfaces even at low concentrations. Details of the clustering method used are available in the SI section 3. Previous STM-BJ reports on molecules with amine, thioether and thiol contacts at a concentration of 1 mM demonstrated JFPs of 27, 42 and 75% respectively.[38] For molecule **6** at a concentration 1000-fold lower, junctions are still observed at a probability significantly higher than this previous report. For this to be the case significant accumulation of molecules from solution on to the surface must occur. Another report demonstrates molecules with pyridine and dihydrobenzo[b]thiophene contacts have 100% JFP with 0.1 mM solutions with additional investigations showing this drops off at lower concentrations.[24] Carbodithioate esters have high junction formation probabilities just as good if not better than the discussed Au–anchor groups.

Compound **12** (**Figure 3**) was also prepared to provide a direct comparison with molecule **2** to evaluate the benefit of adding C=S functionality to a molecule of comparable length and effectively equivalent positioning of the contact groups. **12** was also selected as a single CH_2 is substituted for the carbon of C=S function to give length equivalence for comparison. STM-BJ measurements of **12** shows two overlapping conductance peaks at $10^{-3.64}$ and $10^{-4.05}$ (**Figure 3**) with a very clean break off in excellent agreement with the molecular length. The presence of the C=S in **2** gives a clear mono-distributed conductance profile, and boosts the conductance compared to **12** by approximately an order of magnitude.

This article is protected by copyright. All rights reserved.

10.1002/anie.202403577

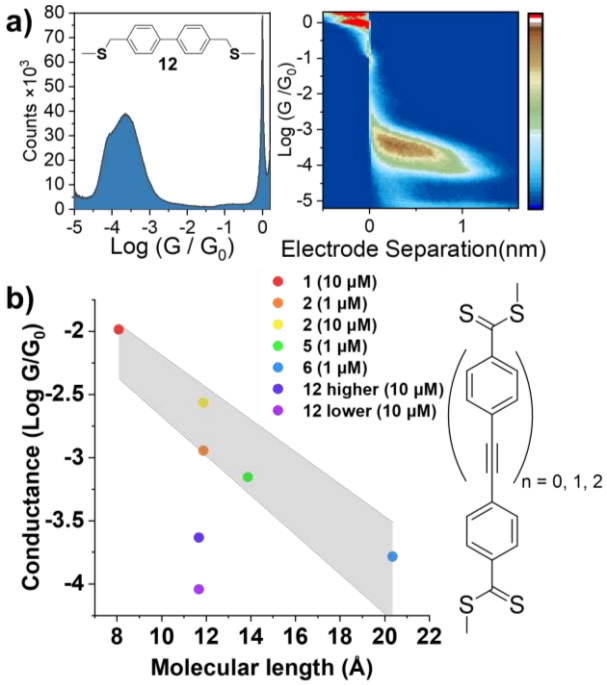

Figure 3. a) STM-BJ measurements of **12** at 300 mV bias in anisole at 10 μM concentration. 20 nm piezo ramp. b) Conductance vs. molecular length for molecules measured in STM-BJ in anisole solvent at 300 mV bias. Linear fit of compounds **1**,**5** & **6** with ± 10% margin gives the grey shade area. Linear fit of **1**,**5**, & **6** used to calculate β value (β = 0.33)

The plot of log(conductance) vs. molecule length shows a clear linear trend for the carbodithioate ester-containing molecule wires. For the quasi-oligomeric series (**1**,**3**,**5**,**6**, see **Figure 3b**) it was not possible to measure the series at the same concentration due to the difficulties in measuring **1**, where 10 μM was the only concentration identified where 5000+ traces could be obtained. A ±10% margin of the linear fit of conductance for **1**, **5** & **6**, was used to demonstrate the general trend of conductance vs. molecular length. A β value of 0.33 $Å^{-1}$ for the linear fit is in agreement with data obtained for molecular wires with similar conjugated backbones.[24, 30, 39, 40] The two conductance peaks for molecule **12** fall well outside of the shaded conductance trend for the carbodithioate esters, highlighting how the C=S moiety is significantly involved in electrode contact and charge transport, by providing additional electronic coupling between the molecule and the metallic electrodes, at least when compared to the comparable length unsaturated $MeS(CH_2)$- linker. These measurements on molecule **12** are in good agreement with literature measurements, with **12** showing a lower conductance than our measurements on carbodithioate ester compounds of similar length (**2** and **5**).[41]

This article is protected by copyright. All rights reserved.

15213773, ja, Downloaded from https://onlinelibrary.wiley.com/doi/10.1002/anie.202403577 by Lancaster University, Wiley Online Library on [31/05/2024]. See the Terms and Conditions (https://onlinelibrary.wiley.com/terms-and-conditions) on Wiley Online Library for rules of use; OA articles are governed by the applicable Creative Commons License

Accepted Manuscript

10.1002/anie.202403577

15213773, ja, Downloaded from https://onlinelibrary.wiley.com/doi/10.1002/anie.202403577 by Lancaster University, Wiley Online Library on [31/05/2024]. See the Terms and Conditions (https://onlinelibrary.wiley.com/terms-and-conditions) on Wiley Online Library for rules of use; OA articles are governed by the applicable Creative Commons License

Accepted Manuscript

Table 1 Conductance values and step length values for carbodithioate esters measured in anisole at 300 mV.

Entry (Conc.)	Conductance Log (G/G_0)	Step length (nm)
1 (10 μM)	−1.99	0.36 ± 0.15
2 (10 μM)	−2.57	0.56 ± 0.25
2 (1 μM)	−2.95	0.50 ± 0.25
5 (1 μM)	−3.16	0.52 ± 0.18
6 (1 μM)	−3.79	0.76 ± 0.21
12 (10 μM) upper	−3.64	0.48 ± 0.15
12 (10 μM) lower	−4.05	0.48 ± 0.15

The conductance values in **Table 1** for the carbodithioate ester-containing molecular wires demonstrate that the conductance is highly comparable to other OPE and biphenyl-based molecular wires with other anchoring groups. For example the conductance of **2** is comparable to benzidine[42] and [1,1'-biphenyl]-4,4'-dithiol,[43] but there reports concerning the long-term instability of aromatic amines and thiols.[16] Tolane- and OPE-based molecules **5**–**6** also have comparable conductance with both their thiol,[30] and thiomethylether[44] analogues previously reported. Despite the differences in techniques **6** demonstrates a significantly higher junction formation probability at much lower concentrations than its previously reported thiomethylether counterpart.[45]

Stability study

When introducing a contact group to the research community, it is important to demonstrate that the functionality is at least stable under ambient conditions for orders of magnitude longer in time duration than any typical STM-break junction experiment (2–3 hours on our instruments).To investigate the longer-term stability of the carbodithioate ester functionality, **1** was dissolved in DCM-d_2 and the ^{1}H NMR spectrum was acquired, followed by reacquisition after 13 days of incubation at room temperature (**Figure 4**). In DCM-d_2, **1** remains stable in solution in the presence of oxygen and trace H_2O. This further highlights the benefits of using this functional group, where there is clear evidence that impurities in solutions of the substrates do not form or accumulate over extended periods. It is important to note that no ^{1}H NMR peak line broadening, changes in solution colour or transparency, and no precipitation was observed after 13 days demonstrating that the purity of the compound remains extremely close to that of the sample 13 days prior.

This article is protected by copyright. All rights reserved.

10.1002/anie.202403577

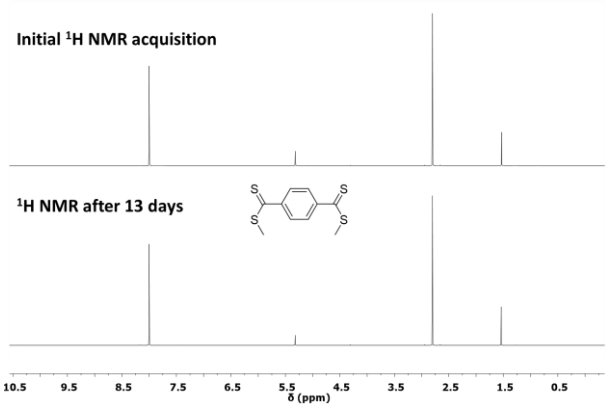

Figure 4 ^{1}H NMR of **1** in DCM-d_2 at 298 K after 0, and 13.05 days in the presence of air and trace H_2O.

Surface Enhanced Raman Spectroscopy (SERS) measurements

To further demonstrate that the carbodithioate esters are clearly interacting with the surface, Raman measurements were performed on powder samples and compared with SERS data acquired from citrate capped gold nanoparticles (CitAuNP, prepared using literature procedure[46]) on silicon substrates where the molecule of interest was drop-casted from a 1 mM toluene solution (**Figure 5**).

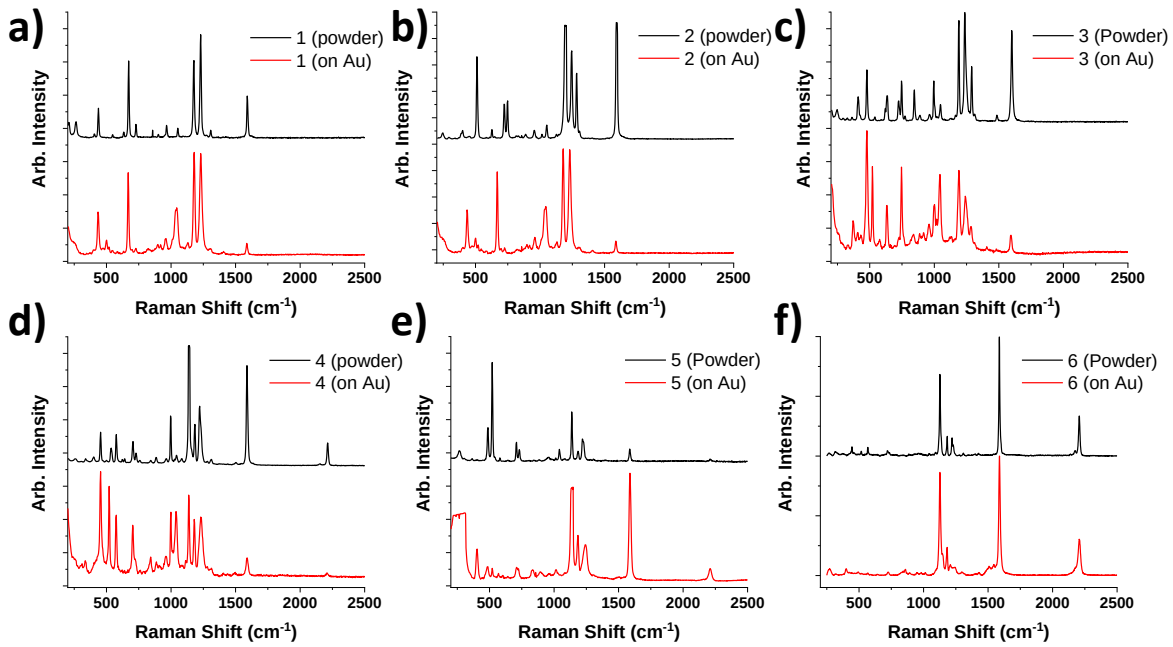

Figure 5. Raman spectroscopy on compounds **1**–**6** as powder on Si substrates and drop-cast (from 1 mM toluene solutions) on to CitAuNPs on silicon substrates. 785 nm laser.

In the Raman data (**Figure 5**), peaks corresponding to vibrational modes of the aromatic backbone of the molecular wires (1600 cm^{-1}) are evident in both the SERS configuration and the powder samples. However, there are some clear changes in relative peak intensities in all

This article is protected by copyright. All rights reserved.

15213773, ja, Downloaded from https://onlinelibrary.wiley.com/doi/10.1002/anie.202403577 by Lancaster University, Wiley Online Library on [31/05/2024]. See the Terms and Conditions (https://onlinelibrary.wiley.com/terms-and-conditions) on Wiley Online Library for rules of use; OA articles are governed by the applicable Creative Commons License

Accepted manuscript

15213773, ja, Downloaded from https://onlinelibrary.wiley.com/doi/10.1002/anie.202403577 by Lancaster University, Wiley Online Library on [31/05/2024]. See the Terms and Conditions (https://onlinelibrary.wiley.com/terms-and-conditions) on Wiley Online Library for rules of use; OA articles are governed by the applicable Creative Commons License

Accepted Manuscript

examples. For instance, in the spectra for **2**, the peak at 1600 cm^{-1} and the peaks at ≈1150–1250 cm^{-1} have similar relative intensities when acquired with the powder material. In contrast, spectra for **2** in SERS configuration show the peak at 1600 cm^{-1} with significantly reduced intensity relative to the peaks at ≈1150–1250 cm^{-1}. Such changes in intensity are typical of molecules binding to a surface and being in a different orientation compared to the average orientation in the powder sample, with some modes enhanced by the SERS configuration, and other suppressed due to selection rules. There are several examples across the series of **1–6** where spectra look 'similar' from powder vs. SERS, but nevertheless there are large changes in relative intensities and some subtle shifts in the peaks which are indicative of surface binding. A peak at 1195 cm^{-1} (assigned as C=S stretch)[47] is present throughout all spectra and typically has high intensity either as powder or drop cast sample. This indicates that the C=S functionality is remaining intact when bound on to the Au nanoparticle surface.

Gap mode Raman studies with 2

To further investigate the interaction of the $–CS_2Me$ functionality with the substrate, gap mode Raman spectroscopic characterisation has been performed with compound **2** on flame annealed gold slides. Gap mode Raman spectroscopy involves adsorbing gold nanoparticles on top of target monolayers assembled on a planar substrate: the excitation of gap-mode plasmons greatly enhance the Raman scattering and allow the recording of good quality spectra from monolayers absorbed on smooth metal surfaces.[48] Gold slides were immersed in a 1 mM toluene solution of **2** for 24 hours and were rinsed thoroughly with toluene. The slide was then immersed in an aqueous solution of AuCitNPs for 1 h and was rinsed with water and methanol, and allowed to dry. Raman results (**Figure 6**) show that despite copious rinsing with solvents that easily dissolve **2**, a strong Raman signature similar to that observed with drop cast solutions was obtained, confirming substantial Raman enhancement in the gap mode samples with **2** remaining bound to the surface. The spectra are generally similar across the nine areas measured in SERS configuration. The peak at 1600 cm^{-1} has a high intensity as an ultra-thin layer in the gap mode measurements, in contrast to the drop cast samples. This suggests an alternative molecular arrangement in the gap mode measurements with **2** absorbed on a flat surface compared to bulk measurements on dropcast CitAuNPs where rougher surface morphology will be present. The C=S stretching peak is also present in the gap mode measurements and is particularly strong in intensity compared to neighbouring peaks.

This article is protected by copyright. All rights reserved.

10.1002/anie.202403577

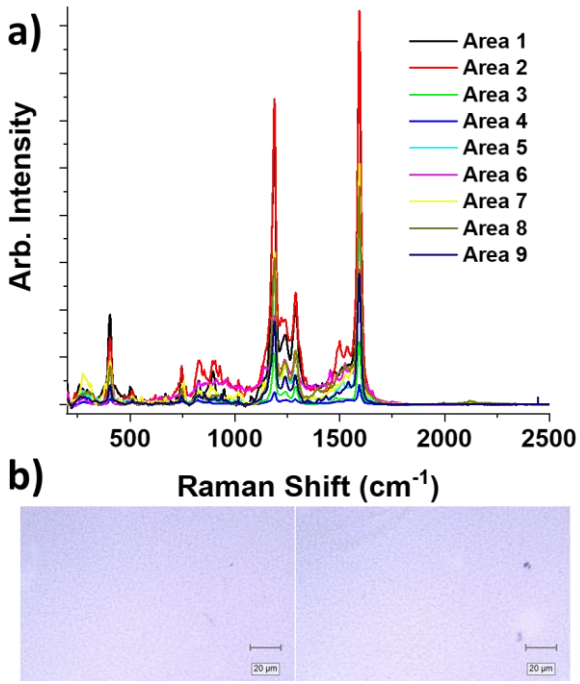

Figure 6. a) Surface enhanced Raman spectrum of GAP mode samples of **2** on gold slides with CitAuNPs. b) Optical images of gold slides at 50× magnification on confocal microscope showing the array of CitAuNPs fixed on the gold slide by the layer of **2** on the Au surface.

Selected XPS studies with 2

To further support the Raman studies, XPS studies were conducted on molecule **2** as both powder samples and SAMs on gold on mica slides (prepared the same as for gap mode studies above). The XPS data (Figure S27) shows clear evidence for gold binding with new S 2p doublets associated with the binding to Au in the SAM sample with evidence of preferential C=S binding due to a reduction in peak area associated with the C=S functionality. Full details of the XPS peak assignment is provided in SI section 7.2

Complexation of Carbodithioate ester with Au^{I}

The solution stability studies (**Figure 4**) show that the carbodithioate ester functionality remains intact under ambient conditions, but this raises the question: what happens in the presence of Au? To address this, Au^{I} complex **14** was prepared from commercially available Au^{I} precursor (**Figure 7**). Analogous ethyl carbodithioate ester complexes have been prepared previously by Butenschön and co-workers for other applications and show the ester remains intact while coordinated to the electron deficient Au^{I} metal centre.[49] The complexation study was carried out with an Au(I) gold atom to represent an electron deficient gold atom. i.e. an atom where electron donation from a ligand is highly favorable. At the apex of a gold tip in STM-breakjunction the gold atom(s) here are highly undercoordinated and are more electron

This article is protected by copyright. All rights reserved.

15213773, ja, Downloaded from https://onlinelibrary.wiley.com/doi/10.1002/anie.202403577 by Lancaster University, Wiley Online Library on [31/05/2024]. See the Terms and Conditions (https://onlinelibrary.wiley.com/terms-and-conditions) on Wiley Online Library for rules of use; OA articles are governed by the applicable Creative Commons License

Accepted Manuscript

10.1002/anie.202403577

deficient than well-coordinated Au on flat (1,1,1) surfaces. We believe a Au(I) atom therefore well represents the atoms at the apex of a gold tip.

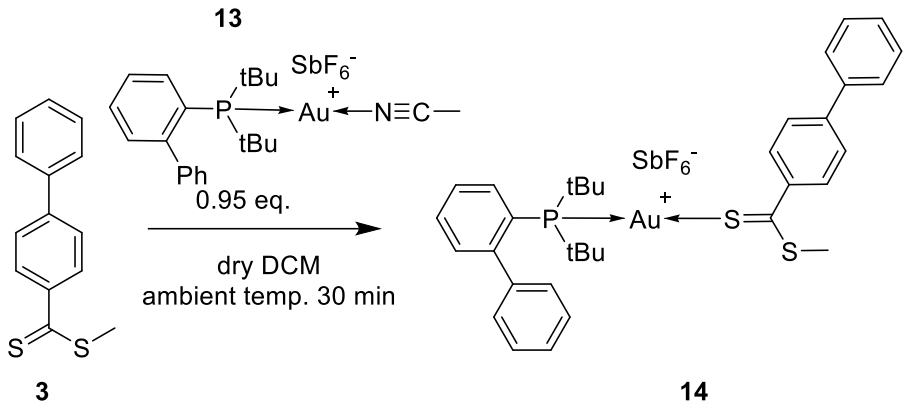

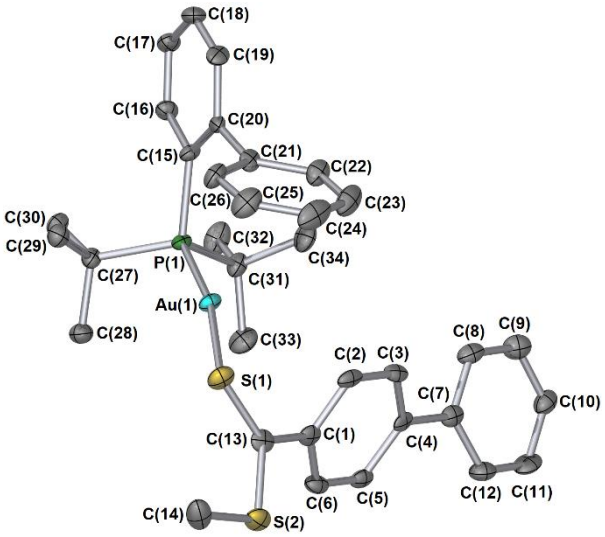

Figure 7 Synthesis of carbodithioate ester-containing Au^{I} complex **14** (top) and X-ray crystallographic structure of **14** crystallised from DCM/hexane (bottom). Ellipsoids shown at 50% probability. Hydrogen atoms and $[SbF_6]^-$ counterion are omitted for clarity. CCDC deposition 2267624.

^{1}H NMR data shows clear evidence for the presence of the carbodithioate ester with the S–Me protons at 3.08 ppm, shifted from 2.81 ppm in uncomplexed ligand **3** (See **Figure S5** and **S20**). The electron deficient Au^{I} centre is responsible for this shift upon coordination. The chemical shift of the C=S carbon shifts from 228.9 ppm to 238.8 ppm upon complexation to the Au^{I} centre.

Crystals of **14** suitable for x-ray diffraction were grown by vapour diffusion from DCM/hexane (**Figure 7**). The X-ray crystallographic structure shows clear evidence for the near linear C=S→Au^{I} interaction. To the best of our knowledge there is no reported X-ray data for such

This article is protected by copyright. All rights reserved.

15213773, ja, Downloaded from https://onlinelibrary.wiley.com/doi/10.1002/anie.202403577 by Lancaster University, Wiley Online Library on [31/05/2024]. See the Terms and Conditions (https://onlinelibrary.wiley.com/terms-and-conditions) on Wiley Online Library for rules of use; OA articles are governed by the applicable Creative Commons License

Accepted Manuscript

15213773, ja, Downloaded from https://onlinelibrary.wiley.com/doi/10.1002/anie.202403577 by Lancaster University, Wiley Online Library on [31/05/2024]. See the Terms and Conditions (https://onlinelibrary.wiley.com/terms-and-conditions) on Wiley Online Library for rules of use; OA articles are governed by the applicable Creative Commons License

Accepted Manuscript

an interaction from a carbodithioate ester (See SI section 5 for CSD search details). We suggest that this C=S→Au interaction is responsible for the boost in conductance observed in **2** compared to **12**, and that the C=S interaction is likely preferred to the C–SMe→Au interaction. Raman spectroscopy was also performed on **14** as a powder sample (See SI **Figure S25**), which shows a highly similar spectral profile to **3** as powder with the typical C=S stretching peak at 1195 cm^{-1}.

Supporting Theoretical Calculations

Density Functional Theory calculations were performed on molecules **1–3** to gain insight into their binding behaviour on the Au surface. The relaxed structures (Figure S31) show that **1–3** are binding relatively upright on the surface, with the SMe contacting a single Au binding site and the C=S bridging two Au atoms. The discussed binding mode likely explains why the calculations (Table S7) yield molecule–Au surface binding energies of 1.37, 1.27 and 1.07 eV for molecules **1–3** respectively, which are very strong for a dative binding group. Interestingly the presence of a second *para*-substituted carbodithioate ester anchor on the other side of the molecule (in **1** and **2**) appears to strengthen the gold–molecule binding energy. This is likely due to the electron withdrawing nature of the carbodithioate ester facilitating more π-backbonding from the Au atoms. The frontier molecular orbitals from these calculations (SI section 8.3) also indicate a strong interaction between the gold surface and the sulfur atoms.

Conclusion

With this study, we have demonstrated that the methyl carbodithioate ester is a suitable neutral contact group for gold in molecular electronics and more importantly, we have verified the stability in air and in contact with Au. We have developed a synthetic protocol that allows the introduction of R-CS_2Me termini in molecular wires through well-known Pd-catalysed C–C cross-coupling reactions. NMR characterisation suggests excellent stability in the presence of water and aerobic oxidants. Raman/SERS, XPS and single-crystal XRD data shows excellent resilience of the R–CS_2Me functionality even in the presence of metallic substrates. To conclude, this work clearly demonstrates that the carbodithioate ester possesses competitive properties across a range of parameters, with good stability, synthetic accessibility, high junction formation probability, spectroscopically defined coordination to gold and competitive conductance values coupled to defined conductance profiles. This justifies the use of this functional group in further studies transitioning towards stable larger area devices.

This article is protected by copyright. All rights reserved.

15213773, ja, Downloaded from https://onlinelibrary.wiley.com/doi/10.1002/anie.202403577 by Lancaster University, Wiley Online Library on [31/05/2024]. See the Terms and Conditions (https://onlinelibrary.wiley.com/terms-and-conditions) on Wiley Online Library for rules of use; OA articles are governed by the applicable Creative Commons License

Accepted Manuscript

ASSOCIATED CONTENT

Synthesis and Characterization is available in the supporting information.

Supporting information is attached as part of this submission.

Raw data is available at https://datacat.liverpool.ac.uk/id/eprint/2481

DOI: 10.17638/datacat.liverpool.ac.uk/2481

Acknowledgments

This work was supported with funding from the Leverhulme Foundation (grant RPG-2019-308). A.V. acknowledges funding from the Royal Society (URF\R1\191241). Dr Nathan Halcovitch is thanked for guidance with the WebCSD search. Durham University Chemistry is thanked for in-kind mass spectrometry measurements of **5** and **6** by ASAP-TOF. Dr Xiaohang Qiao is thanked for supplying some of the Au on mica slides. SB, SPJ, CJL and RJN also gratefully acknowledge funding from EPSRC (grant EP/X026876/1, Quantum engineering of energy-efficient molecular materials, QMol).

TOC graphic

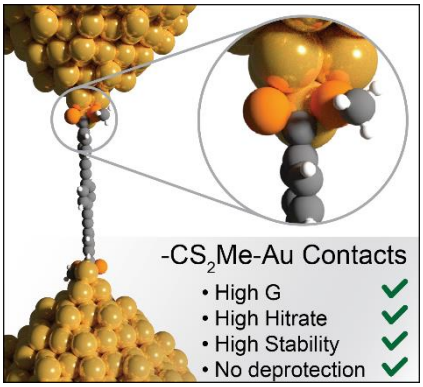

A series of Carbodithioate ester-containing molecular wires have been synthesized and characterized to demonstrate the functionality as a great contact group for molecular electronics with good all-around properties including strong surface binding and high conductance. Raman, XPS and theoretical calculations support the STM-BJ conductance data and rationalize the binding groups' performance through a strong C=S to Au interaction.

Twitter: @WardGroupChem

References

[1] C. Tang, R. T. Ayinla, K. Wang, *J. Mater. Chem. C* **2022**, *10*, 13717-13733.
[2] J. S. Ward, A. Vezzoli, *Curr. Opin. Electrochem.* **2022**, *35*, 101083.
[3] Z. Tan, W. Jiang, C. Tang, L.-C. Chen, L. Chen, J. Liu, Z. Liu, H.-L. Zhang, D. Zhang, W. Hong, *CCS Chemistry* **2021**, *4*, 713-721.
[4] S.-L. Lv, C. Zeng, Z. Yu, J.-F. Zheng, Y.-H. Wang, Y. Shao, X.-S. Zhou, *Biosensors* **2022**, *12*, 565.
[5] T. Miyazaki, Y. Shoji, S. Fujii, T. Fukushima, *Jpn J. Appl. Phys.* **2021**, *60*, 108002.
[6] F. Chen, J. Hihath, Z. Huang, X. Li, N. J. Tao, *Annu. Rev. Phys. Chem.* **2007**, *58*, 535-564.
[7] T. A. Su, M. Neupane, M. L. Steigerwald, L. Venkataraman, C. Nuckolls, *Nat. Rev. Mater.* **2016**, *1*, 16002.

This article is protected by copyright. All rights reserved.

[8] A. Daaoub, J. M. F. Morris, V. A. Béland, P. Demay-Drouhard, A. Hussein, S. J. Higgins, H. Sadeghi, R. J. Nichols, A. Vezzoli, T. Baumgartner, S. Sangtarash, *Angew. Chem. Int. Ed.* **2023**, *62*, e202302150.

[9] F. Chen, X. Li, J. Hihath, Z. Huang, N. Tao, *J. Am. Chem. Soc.* **2006**, *128*, 15874-15881.

[10] F. H. van Veen, L. Ornago, H. S. J. van der Zant, M. El Abbassi, *J. Phys. Chem. C.* **2022**, *126*, 8801-8806.

[11] Z. Xie, I. Bâldea, S. Oram, C. E. Smith, C. D. Frisbie, *ACS Nano* **2017**, *11*, 569-578.

[12] Z. Xie, I. Bâldea, C. D. Frisbie, *J. Am. Chem. Soc.* **2019**, *141*, 18182-18192.

[13] Y. Xue, X. Li, H. Li, W. Zhang, *Nat. Commun.* **2014**, *5*, 4348.

[14] T. Bürgi, *Nanoscale* **2015**, *7*, 15553-15567.

[15] E. Leary, A. La Rosa, M. T. González, G. Rubio-Bollinger, N. Agraït, N. Martín, *Chem. Soc. Rev.* **2015**, *44*, 920-942.

[16] W. Hong, D. Z. Manrique, P. Moreno-García, M. Gulcur, A. Mishchenko, C. J. Lambert, M. R. Bryce, T. Wandlowski, *J. Am. Chem. Soc.* **2012**, *134*, 2292-2304.

[17] W. Haiss, S. Martín, E. Leary, H. v. Zalinge, S. J. Higgins, L. Bouffier, R. J. Nichols, *J. Phys. Chem. C.* **2009**, *113*, 5823-5833.

[18] W. Haiss, R. J. Nichols, H. van Zalinge, S. J. Higgins, D. Bethell, D. J. Schiffrin, *Phys. Chem. Chem. Phys* **2004**, *6*, 4330-4337.

[19] R. J. Nichols, W. Haiss, S. J. Higgins, E. Leary, S. Martin, D. Bethell, *Phys. Chem. Chem. Phys* **2010**, *12*, 2801-2815.

[20] Y. S. Park, A. C. Whalley, M. Kamenetska, M. L. Steigerwald, M. S. Hybertsen, C. Nuckolls, L. Venkataraman, *J. Am. Chem. Soc.* **2007**, *129*, 15768-15769.

[21] M. Gantenbein, X. Li, S. Sangtarash, J. Bai, G. Olsen, A. Alqorashi, W. Hong, C. J. Lambert, M. R. Bryce, *Nanoscale* **2019**, *11*, 20659-20666.

[22] R. Davidson, O. A. Al-Owaedi, D. C. Milan, Q. Zeng, J. Tory, F. Hartl, S. J. Higgins, R. J. Nichols, C. J. Lambert, P. J. Low, *Inorg. Chem.* **2016**, *55*, 2691-2700.

[23] V. Kaliginedi, A. V. Rudnev, P. Moreno-García, M. Baghernejad, C. Huang, W. Hong, T. Wandlowski, *Phys. Chem. Chem. Phys* **2014**, *16*, 23529-23539.

[24] P. Moreno-García, M. Gulcur, D. Z. Manrique, T. Pope, W. Hong, V. Kaliginedi, C. Huang, A. S. Batsanov, M. R. Bryce, C. Lambert, T. Wandlowski, *J. Am. Chem. Soc.* **2013**, *135*, 12228-12240.

[25] J. Liu, X. Zhao, Q. Al-Galiby, X. Huang, J. Zheng, R. Li, C. Huang, Y. Yang, J. Shi, D. Z. Manrique, C. J. Lambert, M. R. Bryce, W. Hong, *Angew. Chem. Int. Ed.* **2017**, *56*, 13061-13065.

[26] H. Ozawa, M. Baghernejad, O. A. Al-Owaedi, V. Kaliginedi, T. Nagashima, J. Ferrer, T. Wandlowski, V. M. García-Suárez, P. Broekmann, C. J. Lambert, M.-a. Haga, *Chem. Eur. J.* **2016**, *22*, 12732-12740.

[27] W. Chen, H. Li, J. R. Widawsky, C. Appayee, L. Venkataraman, R. Breslow, *J. Am. Chem. Soc.* **2014**, *136*, 918-920.

[28] L. F. Oldfield, J. O. M. Bockris, *J. Phys. Chem.* **1951**, *55*, 1255-1274.

[29] J. A. Jacob, S. Naumov, N. Biswas, T. Mukherjee, S. Kapoor, *J. Phys. Chem. C.* **2007**, *111*, 18397-18404.

[30] Y. Xing, T.-H. Park, R. Venkatramani, S. Keinan, D. N. Beratan, M. J. Therien, E. Borguet, *J. Am. Chem. Soc.* **2010**, *132*, 7946-7956.

[31] F. von Wrochem, D. Gao, F. Scholz, H.-G. Nothofer, G. Nelles, J. M. Wessels, *Nat. Nanotechnol.* **2010**, *5*, 618-624.

[32] Z. Li, H. Li, S. Chen, T. Froehlich, C. Yi, C. Schönenberger, M. Calame, S. Decurtins, S.-X. Liu, E. Borguet, *J. Am. Chem. Soc.* **2014**, *136*, 8867-8870.

[33] H. Zhao, J. Wang, Y. Zheng, J. Li, X. Han, G. He, Y. Du, *Angew. Chem. Int. Ed.* **2017**, *56*, 15334-15338.

[34] T.-H. Park, M. J. Therien, *Org. Lett.* **2007**, *9*, 2779-2782.

[35] B. Xu, N. J. Tao, *Science* **2003**, *301*, 1221-1223.

[36] C. Wu, D. Bates, S. Sangtarash, N. Ferri, A. Thomas, S. J. Higgins, C. M. Robertson, R. J. Nichols, H. Sadeghi, A. Vezzoli, *Nano Lett.* **2020**, *20*, 7980-7986.

[37] W. R. T. Barden, S. Singh, P. Kruse, *Langmuir* **2008**, *24*, 2452-2458.

This article is protected by copyright. All rights reserved.

15213773, ja, Downloaded from https://onlinelibrary.wiley.com/doi/10.1002/anie.202403577 by Lancaster University, Wiley Online Library on [31/05/2024]. See the Terms and Conditions (https://onlinelibrary.wiley.com/terms-and-conditions) on Wiley Online Library for rules of use; OA articles are governed by the applicable Creative Commons License

Accepted Manuscript

[38] P. S. Yoo, T. Kim, *Bull. Korean Chem. Soc.* **2015**, *36*, 265-268.
[39] V. Kaliginedi, P. Moreno-García, H. Valkenier, W. Hong, V. M. García-Suárez, P. Buiter, J. L. H. Otten, J. C. Hummelen, C. J. Lambert, T. Wandlowski, *J. Am. Chem. Soc.* **2012**, *134*, 5262-5275.
[40] M. Carlotti, M. Degen, Y. Zhang, R. C. Chiechi, *J. Phys. Chem. C.* **2016**, *120*, 20437-20445.
[41] E. Leary, L. A. Zotti, D. Miguel, I. R. Márquez, L. Palomino-Ruiz, J. M. Cuerva, G. Rubio-Bollinger, M. T. González, N. Agrait, *J. Phys. Chem. C.* **2018**, *122*, 3211-3218.
[42] L. Venkataraman, J. E. Klare, C. Nuckolls, M. S. Hybertsen, M. L. Steigerwald, *Nature* **2006**, *442*, 904-907.
[43] A. Mishchenko, D. Vonlanthen, V. Meded, M. Bürkle, C. Li, I. V. Pobelov, A. Bagrets, J. K. Viljas, F. Pauly, F. Evers, M. Mayor, T. Wandlowski, *Nano Lett.* **2010**, *10*, 156-163.
[44] D. Miguel, L. Álvarez de Cienfuegos, A. Martín-Lasanta, S. P. Morcillo, L. A. Zotti, E. Leary, M. Bürkle, Y. Asai, R. Jurado, D. J. Cárdenas, G. Rubio-Bollinger, N. Agraït, J. M. Cuerva, M. T. González, *J. Am. Chem. Soc.* **2015**, *137*, 13818-13826.
[45] C. Zhan, G. Wang, X.-G. Zhang, Z.-H. Li, J.-Y. Wei, Y. Si, Y. Yang, W. Hong, Z.-Q. Tian, *Angew. Chem. Int. Ed.* **2019**, *58*, 14534-14538.
[46] J. F. Li, X. D. Tian, S. B. Li, J. R. Anema, Z. L. Yang, Y. Ding, Y. F. Wu, Y. M. Zeng, Q. Z. Chen, B. Ren, Z. L. Wang, Z. Q. Tian, *Nat. Protoc.* **2013**, *8*, 52-65.
[47] A. C. Storer, Y. Ozaki, P. R. Carey, *Can. J. Chem.* **1982**, *60*, 199-209.
[48] K. Ikeda, N. Fujimoto, H. Uehara, K. Uosaki, *Chem. Phys. Lett.* **2008**, *460*, 205-208.
[49] S.-F. Schmiel, H. Butenschön, *Eur. J. Org .Chem.* **2021**, *2021*, 2388-2401.

This article is protected by copyright. All rights reserved.

15213773, ja, Downloaded from https://onlinelibrary.wiley.com/doi/10.1002/anie.202403577 by Lancaster University, Wiley Online Library on [31/05/2024]. See the Terms and Conditions (https://onlinelibrary.wiley.com/terms-and-conditions) on Wiley Online Library for rules of use; OA articles are governed by the applicable Creative Commons License

Accepted Manuscript